

WEAKLY NONLINEAR DESCRIPTION OF PARAMETRIC INSTABILITIES IN VIBRATING FLOWS

E. Knobloch, Department of Physics, University of California, Berkeley CA 94720, USA,
knobloch@physics.berkeley.edu, J. M. Vega, E.T.S.I. Aeronauticos, Universidad Politecnica de Madrid, 28040
Madrid, Spain, vega@fmetsia.upm.es

Introduction

This project focuses on the effects of weak dissipation on vibrational flows in microgravity and in particular on (a) the generation of mean flows through viscous effects and their reaction on the flows themselves, and (b) the effects of finite group velocity and dispersion on the resulting dynamics in large domains. The basic mechanism responsible for the generation of such flows is nonlinear and was identified by Schlichting [21] and Longuet-Higgins [14]. However, only recently has it become possible to describe such flows self-consistently in terms of amplitude equations for the parametrically excited waves coupled to a mean flow equation. The derivation of these equations is nontrivial because the limit of zero viscosity is singular. This project focuses on various aspects of this singular problem (i.e., the limit $C \equiv \nu(g h^3)^{-1/2} \ll 1$, where ν is the kinematic viscosity and h is the liquid depth) in the weakly nonlinear regime. A number of distinct cases is identified depending on the values of the Bond number, the size of the nonlinear terms, distance above threshold and the length scales of interest. The theory provides a *quantitative* explanation of a number of experiments on the vibration modes of liquid bridges and related experiments on parametric excitation of capillary waves in containers of both small and large aspect ratio. The following is a summary of results obtained thus far.

Surface-wave damping in a brimful circular cylinder [19]

Henderson and Miles [6] discovered a substantial discrepancy between the measured decay rate of free oscillations of a brimful circular cylinder and theoretical predictions based on leading order asymptotics in powers of $C^{1/2}$, $C = \nu(g R^3)^{-1/2}$, where R is the radius of the cylinder. At the same time they found good agreement between the measured and predicted frequencies. The resolution of this discrepancy follows from the observation by Higuera et al [7] and Martel and Knobloch [17] that under typical conditions the $\mathcal{O}(C)$ term in the expansion of the damping rates $\text{Re}(s)$ of capillary and gravity-capillary waves is comparable to the leading order term.

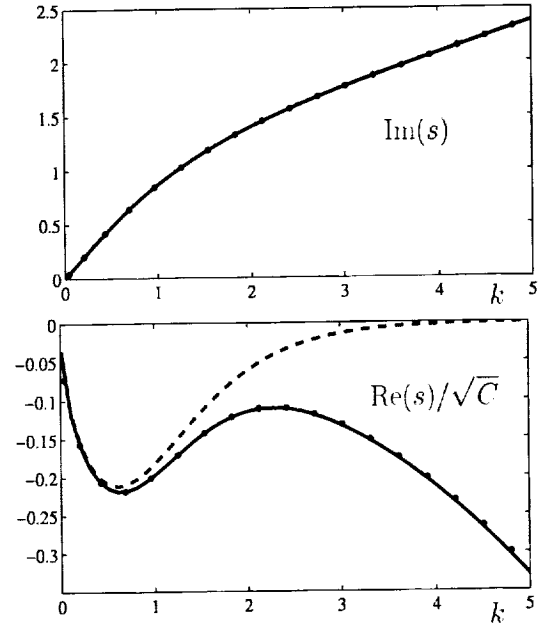


Figure 1: The gravity-capillary modes for $k = \mathcal{O}(1)$. The dots indicate the exact solution; asymptotic results through $\mathcal{O}(C^{1/2})$ and $\mathcal{O}(C)$ are indicated by dashed and solid lines, respectively.

This is so despite the fact that C is typically small, $C \approx 10^{-4}$. Fig. 1 shows what happens in a horizontally infinite layer of depth h [17]. The figure shows the decay rate $\text{Re}(s)$ and frequency $\text{Im}(s)$ as a function of the wavenumber k , nondimensionalized using h^{-1} , for the parameter values used in [6]: $B \equiv \rho g h^2 / \sigma = 1.96 \cdot 10^2$ and $C \equiv \nu(g h^3)^{-1/2} = 0.43 \cdot 10^{-4}$. Here σ is the surface tension.

In a cylinder the corresponding calculations are more involved because of viscous boundary layers at the sidewall and the presence of a contact line. We find

$$\text{Re}(s) = C^{1/2} \omega_1 + C \omega_2 + \mathcal{O}(C^{3/2}), \quad (1)$$

$$\text{Im}(s) = \omega_0 - C^{1/2} \omega_1 + \mathcal{O}(C^{3/2}), \quad (2)$$

where the $\mathcal{O}(C^{1/2})$ terms come from viscous dissipation in the oscillatory Stokes boundary layers near the solid wall and bottom of the cylinder, and the $\mathcal{O}(C)$

terms come from (a) viscous dissipation in the bulk and (b) a first correction to the viscous dissipation in the Stokes boundary layers. The neglected $\mathcal{O}(C^{3/2})$ includes viscous dissipation in the oscillatory boundary layer at the free surface. We find that ω_2/ω_1 for typical Bond numbers $B = \rho g R^2 / \sigma$ and aspect ratios $\Lambda = h/R$ is quite large even for the fundamental mode and increases with the mode number. As a result the $\mathcal{O}(C)$ term in s is important and its omission leads to errors that increase with the mode number, as found in [6]. The absence of this term in ω implies that the leading order approximation for the frequencies is much better than the corresponding approximation for the damping rates. The computation of the $\mathcal{O}(C)$ terms requires care because of a singularity in the expansion at the (pinned) contact line. The theoretical damping rates (1) are compared with measured rates in Table 1, and demonstrate a substantial improvement over the $\mathcal{O}(C^{1/2})$ results of [6].

The brimful cylinder is ideal for understanding the effects of dissipation in boundary layers because the meniscus is pinned to the brim, thereby eliminating unknown effects arising from the dynamics of the meniscus. In addition the absence of corners in the container makes the boundary layer structure uniform and relatively simple. The damping rate calculation lends us confidence that we have correctly identified the major source of discrepancy between existing theory and experiment and that we know how to correct the theory, at least in cases in which surface contamination and contact angle dynamics can be ignored. It follows that (the bulk of the) dissipation in clean-surface experiments is accounted for by the classical Navier-Stokes formulation and is not due to unknown dissipation mechanisms in the meniscus or air-water interface. In particular any residual discrepancy between theory and experiment can now be used as a diagnostic for the presence of contamination. This fact has triggered a new experimental effort to measure damping rates of gravity-capillary waves in finite domains by M. Schatz (private communication). In addition the calculation forms the basis for future nonlinear studies of gravity-capillary waves in cylinders and their interactions.

Chaotic oscillations in a nearly inviscid axisymmetric capillary bridge at 2 : 1 resonance [16]

This paper considers a liquid bridge in microgravity supported between two disks vibrating at two frequencies close to 2 : 1 resonance. Under appropriate conditions this vibration excites the corresponding natural vibra-

(m, q)	Experiment		Approximation		Theory	
	f	Δ	f_1	Δ_1	f_2	Δ_2
(1, 0)	4.65	1.4	4.66	1.13	4.67	1.37
(2, 0)	6.32	1.8	6.32	1.24	6.34	1.75
(0, 1)	6.84	1.2	6.73	0.44	6.85	0.95
(3, 0)	7.80	2.2	7.79	1.29	7.82	2.11
(1, 1)	8.57	1.5	8.57	0.48	8.59	1.45
(4, 0)	9.26	2.4	9.24	1.32	9.27	2.47

Table 1: Comparison between theory and the experiment [6]. Here f_j is the dimensional frequency (in Hz) to $\mathcal{O}(C^{1/2})$ ($j = 1$), to $\mathcal{O}(C)$ ($j = 2$), with Δ_j the corresponding nondimensional damping rates. m and q are the azimuthal and radial wavenumbers, respectively. After [19].

tion modes (assumed axisymmetric) and these interact nonlinearly. In the nearly inviscid limit $C \ll 1$ this interaction is described by a pair of amplitude equations whose structure depends on the parity of the excited modes. Specifically, if the displacement of the disks follows $z = \pm \Lambda + h_{\pm}(t)$, where

$$h_{\pm}(t) = \mu[\beta_1^{\pm} \exp(i(\Omega_1 + \delta\omega_1)t) + \beta_2^{\pm} \exp(i(\Omega_2 + \delta\omega_2)t)],$$

$\mu \ll 1$, $\Omega_2 = 2\Omega_1$, then the equations for the evolution of the amplitudes of the two competing modes take the form ($k = 1, 2$)

$$\begin{aligned} \epsilon \delta A_{k\tau} &= -(1+i)\alpha_{4k}\sqrt{C} + \alpha_{5k}C - i\alpha_{3k}(\delta)A_k \\ &+ i\alpha_{2k}\epsilon^2 N_k + i\mu(\alpha_{1k}^+ \beta_k^+ - \alpha_{1k}^- \beta_k^-) + \dots \end{aligned} \quad (3)$$

Here $\tau = \delta t$, $\Lambda = \Lambda_0 + \delta\ell$, $\delta \ll 1$, $\beta_k^{\pm}, \omega_k, \ell = \mathcal{O}(1)$ and if the mode A_2 is even in z , $N_1 = A_2 \bar{A}_1$, $N_2 = A_1^2$. This occurs at $\Lambda_0 \approx 0.249$ and $\Lambda_0 \approx 2.23$. At each of these values two natural oscillation modes with frequencies in 2 : 1 ratio are present; it is these modes that are driven by the vibration of the two disks. Finally ϵ measures the amplitude of the two modes. On the other hand, if A_2 is odd in z the nonlinearities are of third order, and $N_k = i\epsilon(\alpha_{2k1}|A_1|^2 + \alpha_{2k2}|A_2|^2)A_k$, $k = 1, 2$.

All the coefficients appearing in Eqs. (3) have been computed from the equations of motion, including the important (but formally subdominant) terms α_{5k} . These calculations require the computation of the contributions from the Stokes boundary layers at the disks, the interface boundary layer, the two corner tori near the edge of the disks and from the bulk. Because of the assumption $C \ll 1$ all nonlinear terms are purely imaginary. The presence of the inhomogeneous terms in

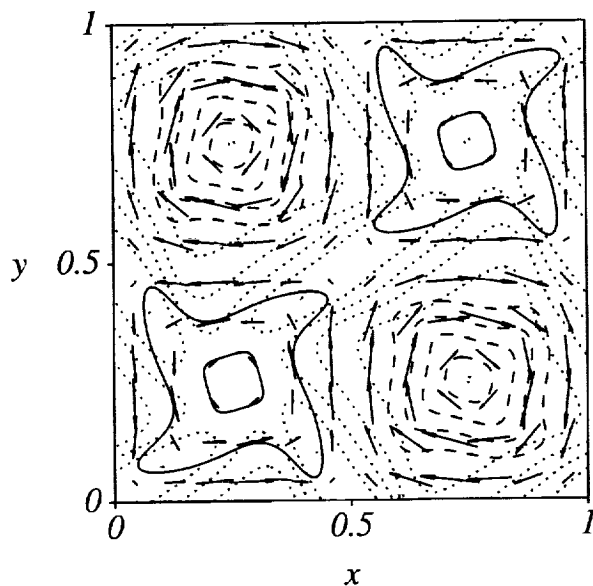


Figure 2: Contour plot of the non-oscillatory components of the film thickness (dotted), vorticity Ω (solid for $\Omega > 0$, dashed for $\Omega < 0$) and velocity arrows for an ordered state. From [25].

Eqs. (3) implies that new phenomena are present that are not captured by standard treatments of the 2 : 1 resonance [12, 9]. Both cases have been analysed, and the results used to make a number of predictions about the sub- and superharmonic response of a liquid bridge subjected to this type of excitation under experimentally relevant conditions. The ensuing chaotic oscillations have been studied numerically and characterized using numerically determined Liapunov exponents.

Quasi-steady vortical structures in vertically vibrating soap films [25]

In a recent paper Afenchenko et al [1] describe the results of an experimental study of flows in vertically vibrated soap films; in this experiment the frame holding the film was rigidly and symmetrically attached to the lateral wall of a closed cavity, which was vibrated vertically. These vortical structures (first reported by Taylor [24]) are similar to ones described by Airiau [2], who excited the film using a loudspeaker fitted to the bottom of the cavity, which was otherwise open. We have examined in detail the possible mechanisms that could lead to the generation of such flows, with special emphasis on those effects that are independent of the shape of the frame supporting the film, of the attachment mode (i.e., the size of the meniscus), and of the excitation process.

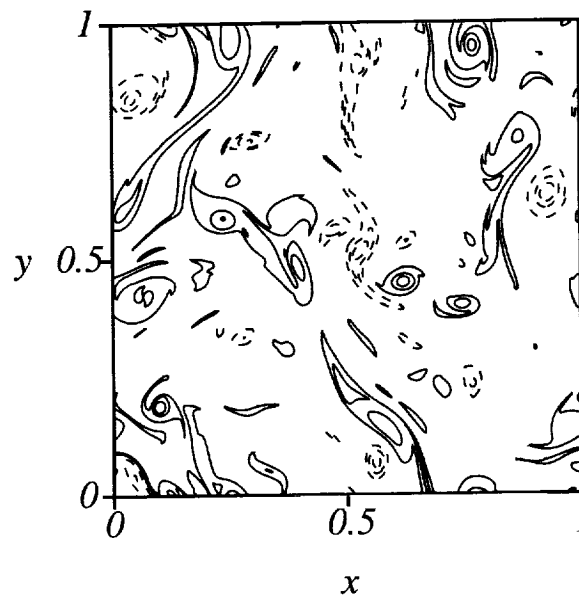


Figure 3: Vorticity contours for a spatially disordered state. From [25].

Thus we focus on those effects that are present in any experiment, e.g., in [1, 2]. In this theory the observed vortical structures are a consequence of the oscillatory tangential and normal stresses on the film due to the surrounding air. The air also damps out Marangoni waves. Because of nonlinearities these stresses (and the inertia of the film) produce non-oscillatory deflection of the film, variation in its thickness, and forcing terms that combine to produce a streaming flow in the film. Coupled evolution equations for these quantities are derived. When the excitation frequency is close to an eigenfrequency of a Marangoni mode of the soap film, the dominant forcing in these equations arises from the nonlinear hydrodynamics within the film volume, while both volume forcing and surface forcing by air are important when there is no resonance with a Marangoni mode. The computed vortex patterns (see Figs. 2,3) agree qualitatively with the experiments.

Compressional modes in parametrically driven Faraday waves in an annulus [18]

Experiments by Douady et al [4] on parametrically driven water waves in an annulus ($C = 4.4 \cdot 10^{-4}$, $B = 8.9$) reveal the presence of a secondary instability of a uniform pattern of standing waves (SW) in the form of an oscillatory *compression* mode (CM). We develop a theory describing this observation based on

(suitably modified) nonlocal amplitude equations for the subharmonic response of the system of the type derived by Knobloch and De Luca [10] for traveling wave convection and Alvarez-Pereira and Vega [3] for pulsating flames, with the nonlinear coefficients deduced from Hansen and Alstrom [5]:

$$A_t = (-1 + i\nu)A + \mu\langle\bar{B}\rangle + iA(\beta|A|^2 + \gamma\langle|B|^2\rangle) + i\alpha A_{xx} \quad (4)$$

$$B_t = (-1 + i\nu)B + \mu\langle\bar{A}\rangle + iB(\beta|B|^2 + \gamma\langle|A|^2\rangle) + i\alpha B_{xx}, \quad (5)$$

subject to the periodic boundary conditions $A(x+1, t) = A(x, t)$, $B(x+1, t) = B(x, t)$. Here $\langle\cdots\rangle$ represents a spatial average over $0 \leq x < 1$. These equations describe the slow temporal evolution of the amplitudes of left- (A) and right-traveling (B) waves in their comoving frames, and provide an asymptotic description of the system sufficiently close to threshold of the Faraday instability that the envelope dynamics are dominated by advection at the group velocity of the waves. A description of this type is appropriate in the weak dissipation limit in which the natural modes of the unforced system, left and right-traveling waves, decay slowly. For this reason the coefficients of the cubic terms are purely imaginary. In the first instance we ignore the presence of viscosity-generated mean flows and study the resulting nonlocal equations. Within this description the onset of the compression mode is described as a secondary pitchfork bifurcation from SW with eigenvector that breaks the SW reflection symmetry. We show that such CM are described by steady but nonuniform solutions of the nonlocal equations with periodic boundary conditions (appropriate to an annular cell) and are present for experimental parameter values. We explore the transition from this mode and identify consecutive bifurcations to nonsteady but uniform states, and to states with complex spatio-temporal dynamics (Fig. 4), some of which are strongly hysteretic. Future work will include viscosity-driven mean flows with self-consistent coupling to the amplitude equations and explore the dynamics of the resulting system of equations. Such mean flows are present not only in large aspect ratio annuli but also in smaller systems, and hence are relevant to the experiments.

A related investigation of the corresponding problem with exact or broken D_4 symmetry is under way, motivated by the Faraday problem in a square or nearly square container. In a container with exact square symmetry two modes related by a 90° rotation are exactly degenerate; this degeneracy is broken if the container is slightly rectangular. Simonelli and Gollub [22] found

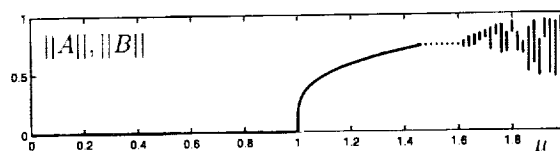


Figure 4: Stable solutions of Eqs. (4,5) for $\nu = 0$, $\beta = 3$, $\gamma = -1$, $\alpha = 0.1$, showing SW ($0 < \mu < 1.46$), CM ($1.46 < \mu < 1.62$) and complex states ($\mu > 1.62$).

no time-dependent dynamics associated with the resulting mode interaction in a square domain. However in a slightly rectangular container they observed periodic and chaotic bursts very close to onset. The real parts of the necessary cubic coefficients are being calculated to leading order in $\mathcal{O}(C)$ together with the mean flows generated in these two geometries. A self-consistent inclusion of such flows offers the possibility of providing the first quantitative description of this interesting behavior. An explanation along the lines described in the next section for the presence of bursts is anticipated.

Bursts [15]

Under appropriate conditions the competition between nearly degenerate Hopf modes with odd and even parity results in dramatic bursting behavior very near the onset of primary instability. This behavior arises in two-dimensional systems of large but finite aspect ratio undergoing an oscillatory instability, or in systems with nearly square symmetry, as discussed by Landsberg and Knobloch [13]. In both cases it is due to the same mechanism.

In a slender system with left-right reflection symmetry (such as a narrow rectangular convection cell) undergoing an oscillatory instability from the trivial state the first two unstable modes typically have opposite parity under reflection. Moreover, because the neutral stability curve for the unbounded system has a parabolic minimum these set in in close succession as the control parameter is increased. We write the perturbation from the trivial state as

$$\Psi(x, y, t) = \epsilon^{\frac{1}{2}} \text{Re} \{ z_+ f_+(x, y) + z_- f_-(x, y) \} + \mathcal{O}(\epsilon),$$

where $\epsilon \ll 1$, $f_{\pm}(-x, y) = \pm f_{\pm}(x, y)$, and y denotes the transverse variables. The complex amplitudes $z_{\pm}(t)$ then satisfy the equations [13]

$$\dot{z}_{\pm} = [\lambda \pm \Delta\lambda + i(\omega \pm \Delta\omega)]z_{\pm} + A(|z_+|^2 + |z_-|^2)z_{\pm} + B|z_{\pm}|^2 z_{\pm} + C\bar{z}_{\pm} z_{\mp}^2. \quad (6)$$

In these equations the nonlinear terms have identical (complex) coefficients because of an approximate *interchange* symmetry between the odd and even modes. The resulting D_4 symmetry [13] is weakly broken whenever $\Delta\lambda \neq 0$ and/or $\Delta\omega \neq 0$, a consequence of the finite aspect ratio of the system. The dynamics in systems with exact D_4 symmetry ($\Delta\lambda = \Delta\omega = 0$) can be shown to take place on a two-dimensional manifold [23] and hence are necessarily simple although the solutions can become unbounded. This is no longer so when the D_4 symmetry is broken. In this case the solutions can experience repeated episodes of dramatic growth followed by collapse but do not become unbounded. The resulting bursts can be periodic or chaotic and set in at a secondary instability very close to onset. To identify such bursts we write

$$z_{\pm} = \rho^{-\frac{1}{2}} \sin\left(\frac{\theta}{2} + \frac{\pi}{4} \pm \frac{\pi}{4}\right) e^{i(\pm\phi + \psi)/2}$$

and introduce a new time-like variable τ defined by $d\tau/dt = \rho^{-1}$. In terms of these variables Eqs. (6) become

$$\begin{aligned} \frac{d\rho}{d\tau} &= -\rho[2A_R + B_R(1 + \cos^2\theta) + C_R \sin^2\theta \cos 2\phi] \\ &\quad - 2(\lambda + \Delta\lambda \cos\theta)\rho^2 \end{aligned} \quad (7)$$

$$\begin{aligned} \frac{d\theta}{d\tau} &= \sin\theta[\cos\theta(-B_R + C_R \cos 2\phi) - C_I \sin 2\phi] \\ &\quad - 2\Delta\lambda \rho \sin\theta \end{aligned} \quad (8)$$

$$\begin{aligned} \frac{d\phi}{d\tau} &= \cos\theta(B_I - C_I \cos 2\phi) - C_R \sin 2\phi \\ &\quad + 2\Delta\omega \rho, \end{aligned} \quad (9)$$

where $A = A_R + iA_I$, etc., together with a decoupled equation for $\psi(t)$. The amplitude of the disturbance is measured by $r \equiv |z_+|^2 + |z_-|^2 = \rho^{-1}$; thus $\rho = 0$ corresponds to infinite amplitude states. Eqs (7-9) show that the restriction to the invariant subspace $\Sigma \equiv \{\rho = 0\}$ is equivalent to taking $\Delta\lambda = \Delta\omega = 0$ in (8,9). The fixed points of the resulting D_4 -symmetric problem correspond to (infinite amplitude) periodic oscillations in time because of the decoupled phase $\psi(t)$. Depending on A , B and C the subspace Σ may contain additional fixed points and/or limit cycles [23]. In our scenario, a burst occurs for $\lambda > 0$ when a trajectory follows the stable manifold of a fixed point (or a limit cycle) $P_1 \in \Sigma$ that is *unstable* within Σ . The instability within Σ then kicks the trajectory towards another fixed point (or limit cycle) $P_2 \in \Sigma$. If this point has an unstable ρ eigenvalue the trajectory escapes from Σ towards a $\rho > 0$ fixed point (or limit cycle), forming a burst. If $\Delta\lambda$ and/or $\Delta\omega \neq 0$ this fixed point may itself be unstable to perturbations of type P_1 and the process then

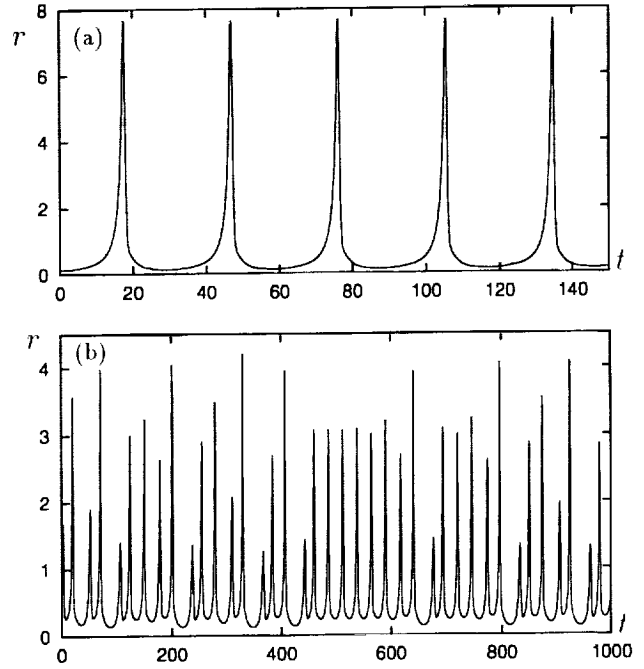


Figure 5: Bursts arising from periodic and chaotic rotations. (a) $\lambda = 0.1$ and (b) $\lambda = 0.072$. The coefficients are $\Delta\lambda = 0.03$, $\Delta\omega = 0.02$, $A = 1 - 1.5i$, $B = -2.8 + 5i$, $C = 1 + i$.

repeats. The scenario thus requires that at least one of the branches in the D_4 -symmetric system be subcritical (P_1) and one supercritical (P_2).

When $\Delta\lambda$ and/or $\Delta\omega \neq 0$ two types of oscillations in (θ, ϕ) are possible: rotations and librations. These oscillations are coupled to excursions in amplitude. Fig. 5 shows a typical sequence of large amplitude bursts arising from repeated excursions towards the infinite amplitude ($\rho = 0$) solutions. The amplitude of these events decreases with increasing $\Delta\lambda$ and their frequency increases, much as found in several experiments. The mechanism outlined here arises naturally in systems with reflection symmetry and appears to be responsible for the regular and irregular bursting exhibited by such systems very close to onset of a primary oscillatory instability.

Dynamics of parametrically modulated dissipative systems in an annulus [11]

Dynamics of parametrically modulated dissipative systems undergoing a symmetry-breaking Hopf bifurcation on a line are explored in full generality, with particular emphasis on the case in which either standing waves or travelling waves are subcritical [20]. The spatially uni-

REFERENCES

form states satisfy equations of the form (cf. Eqs. (4,5))

$$\dot{A} = aA + b\bar{B} + c|A|^2A + d|B|^2A \quad (10)$$

$$\dot{B} = aB + b\bar{A} + c|B|^2B + d|A|^2B. \quad (11)$$

Here a , c and d are complex while b may be taken to be positive. In contrast to Eqs. (4,5) we assume that $\text{Re}(a)$ can pass through zero leading to a spontaneous oscillatory instability, and study the effect of parametric modulation ($b > 0$) on these oscillations. In closely related equations (see Eqs. (6)) bursts occur when one of the branches is subcritical (cf. [8]). We have identified the possible dynamical regimes involving spatially uniform states. These include standing waves and non-symmetric mixed modes phase-locked to the drive and interactions between them. The effects of group velocity and dispersion on the stability properties of the spatially uniform states identified above are being analyzed. As a result a number of new instabilities leading, for example, to compression-like states have been described and these lead to various novel spatially inhomogeneous states.

Acknowledgements

This work was supported by NASA under grant UGS97-0308 and by NSF under grant DMS-9703684. We are grateful to F. Higuera, M. Higuera, F. Mancebo, C. Martel, J. Moehlis and J. Nicolas for their assistance in developing the projects described above, and to P. Weidman for making his experimental results available prior to publication.

References

- [1] V.O. Afenchenko, A.B. Ezersky, S.V. Kiyashko, M.I. Rabinovich and P.D. Weidman, *Phys. Fluids*, in press.
- [2] M. Airiau, DEA Report, Ecole Normale Supérieure, Paris (1986).
- [3] C. Alvarez-Pereira and J.M. Vega, *Euro. Jnl. of Appl. Math.* **3**, 55 (1992).
- [4] S. Douady, S. Fauve and O. Thual, *Europhys. Lett.* **10**, 309 (1989).
- [5] P.L. Hansen and P. Alstrom, *J. Fluid Mech.* **351**, 301 (1997).
- [6] D.M. Henderson and J.W. Miles, *J. Fluid Mech.* **275**, 285 (1994).
- [7] M. Higuera, J.A. Nicolas and J.M. Vega, *Phys. Fluids* **6**, 438 (1994).
- [8] P.C. Hirschberg and E. Knobloch, *Physica D* **90**, 56 (1996).
- [9] D.W. Hughes and M.R.E. Proctor, *J. Fluid Mech.* **244**, 583 (1992).
- [10] E. Knobloch and J. DeLuca, *Nonlinearity* **3**, 575 (1990).
- [11] E. Knobloch, C. Martel, J. Moehlis and J.M. Vega, in preparation.
- [12] E. Knobloch and M.R.E. Proctor, *Proc. R. Soc. London A* **415**, 61 (1988).
- [13] A.S. Landsberg and E. Knobloch, *Phys. Rev. E* **53**, 3579 (1996).
- [14] M.S. Longuet-Higgins, *Phil. Trans. R. Soc. London A* **245**, 535 (1953).
- [15] J. Moehlis and E. Knobloch, *Phys. Rev. Lett.*, in press.
- [16] F.J. Mancebo, J.A. Nicolas and J.M. Vega, *Phys. Fluids*, in press.
- [17] C. Martel and E. Knobloch, *Phys. Rev. E* **56**, 5544 (1997).
- [18] C. Martel, E. Knobloch and J.M. Vega, in preparation.
- [19] C. Martel, J.A. Nicolas and J.M. Vega, *J. Fluid Mech.* **360**, 213 (1998).
- [20] H. Riecke, J.D. Crawford and E. Knobloch, in *NATO ASI Series B* **237**, 61 (1991).
- [21] H. Schlichting, *Z. Phys.* **33**, 327 (1932).
- [22] F. Simonelli and J.P. Gollub, *J. Fluid Mech.* **199**, 471 (1989).
- [23] J.W. Swift, *Nonlinearity* **1**, 333 (1988).
- [24] S. Taylor, *Proc. R. Soc. London* **27**, 71 (1878).
- [25] J.M. Vega, F.J. Higuera and P.D. Weidman, *J. Fluid Mech.*, in press.